Simultaneous Measurement of Strain and Temperature Based on Clover Microstructured Fiber Loop Mirror

R. A. Perez-Herrera[1a], R. M. André[b], S. F. Silva[b], M. Becker[c], K. Schuster[c], J. Kobelke[c], M. Lopez-Amo[a], J. L. Santos[b] and O. Frazão[b]
[a]Dept. of Electric and Electronic Engineering, Universidad Pública de Navarra, Campus Arrosadia S/N, E-31006, Pamplona, Spain
[b]INESC Porto, Rua do Campo alegre 687 Porto, Portugal
[c]Institute of Photonic Technology (IPHT), Albert-Einstein-Str. 9, 07745 Jena, Germany

ABSTRACT

In this work, an all-fiber loop mirror using a clover microstructured fiber for the simultaneous measurement of temperature and strain is presented. The sensing head is formed by a short piece of clover microstructured fiber with 35 mm length. The geometry of the fiber allowed observing different interferences created by the microstructured fiber core section. Different sensitivities to temperature and strain were obtained and, using a matrix method, it is possible to discriminate both physical parameters. Resolutions of ±2ºC and ±11 με, for temperature and strain, respectively, were attained.

Keywords: Interferometers, fiber optic sensors, multimode interference, photonic crystal fibers.

1. INTRODUCTION

Fiber Loop Mirrors (FLMs) are very attractive structures to be used in several applications such as wavelength filters and sensors [1]–[3]. In a FLM, two interfering waves counter-propagate through the same fiber and are exposed to the same environment. FLMs made of highly birefringent fiber (HiBi-FLM) have several advantages, including input polarization independence and high extinction ratio. Besides the gyroscope application, various kinds of sensors based on FLMs have been realized [3], such as temperature sensors [2], [4], strain sensors [5], [6], pressure sensors, liquid level sensors [7], biochemical sensors, UV detection [8] and multiparameter measurement [9]–[11].

In this work, a length of clover microstructured fiber with a central rectangular silica region containing an air hole defect is inserted into a fiber loop mirror configuration. Four disctint interferometric contributions are generated by this structure associated with the presence of two embedded cores combined with birefringence. This configuration has been characterized in strain and temperature showing different sensitivities.

2. EXPERIMENTAL RESULTS

2.1 Experimental setup

Figure 1 shows the experimental setup containing a broadband light source (BBS), a fiber loop mirror (FLM) and an Optical Spectrum Analyzer (OSA) with 0.1 nm resolution. The broadband light used to illuminate the sensing head has 100 nm in bandwidth at the 1550 nm window.

The FLM was formed by a 3dB optical coupler with low insertion loss and a small clover microstructured fiber section with 35 mm length that was spliced in the two output ports. Two polarization controllers (PC1 and PC2) were also applied to control the interference obtained by the fiber.

The clover microstructured fiber, with a diameter of ~200 μm, was fabricated at IPHT and presents four holes, each one with a diameter of about ~30 μm. Defined by these holes there is a central silica region, approximately rectangular (~

[1] rosa.perez@unavarra.es; phone +34 948 169 328; fax +34 948 169 720;

OFS2012 22nd International Conference on Optical Fiber Sensors, edited by
Yanbiao Liao, Wei Jin, David D. Sampson, Ryozo Yamauchi, Youngjoo Chung, Kentaro Nakamura, Yunjiang Rao,
Proc. of SPIE Vol. 8421, 84216W · © 2012 SPIE · CCC code: 0277-786/12/$18 · doi: 10.1117/12.968585

15.2×11.82 μm^2), with an inside rectangular air-hole with dimensions of ~ 6.76×3.38 μm^2. This air feature has a size that turns it more than a defect in the light propagation along the silica region, fairly splitting it in two cores. This was confirmed by a theoretical analysis of the light propagation in the structure, as shown in Fig 1(b). Indeed, the light field is mostly concentrated in these cores, with some variation depending on the polarization of light. Therefore, this guiding structure exhibits birefringence. The consequence of these features when the fiber is inserted in the loop mirror is a birefringence interferometer associated with each core, i.e., the presence of four disctint interferometric contributions for the output signal.

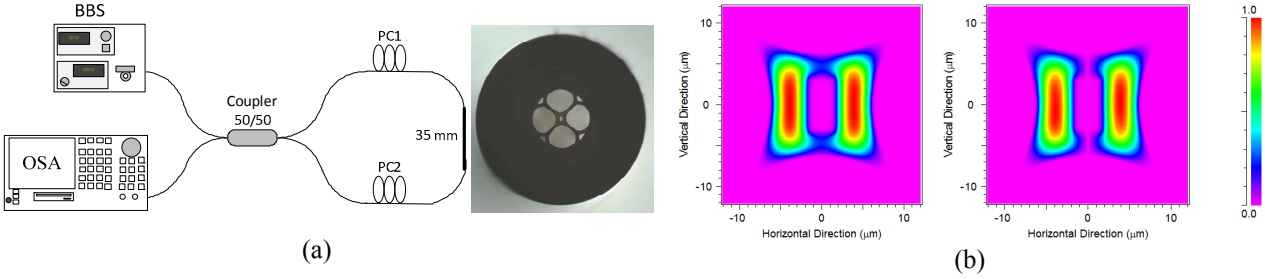

Fig. 1. (a) Schematic diagram of the sensing system (a photograph of the clover microstructured fiber is also shown). (b) modeling of the light propagation in the microstructured fiber for two orthogonal polarizations.

2.2 Results

Fig. 2 illustrates the spectral response of the fiber loop sensor structure. As expected, it is a complex one in face of the several interference terms, originating beating phenomena. The fringes identified in Figure as λ_L are associated with the standard fiber loop mirror channeled spectrum, while λ_B is attributed to birefringence effects. Indeed, it was calculated this microstructured fiber to have a birefringence of ~10^{-4} and, due to the reduced fiber length, only one peak is observed in the wavelength range 1500-1600 nm. Also, it was observed the feature λ_B be highly sensitive to the polarization state of the light. The presence of two cores introduces the extra degrees of freedom responsible for the additional beating effects observed in Fig. 2.

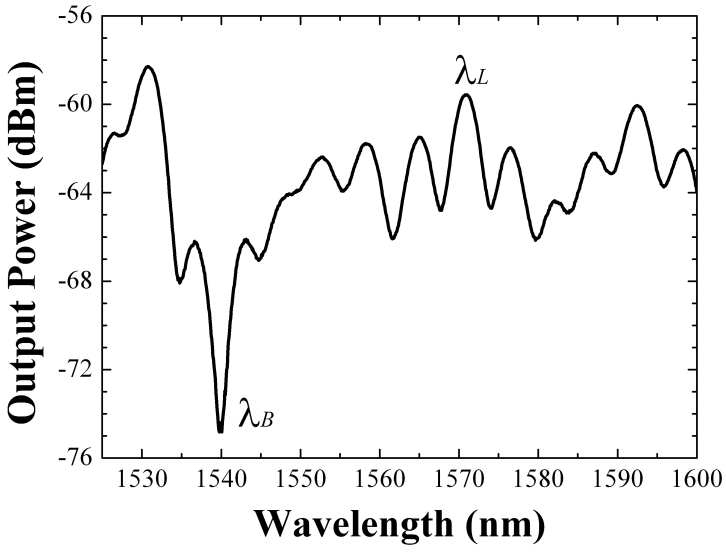

Fig. 2. Output spectrum response of the fiber loop sensing structure.

This structure was characterized in strain at room temperature and also in temperature when no strain is applied. Fig. 3 shows the spectral shift of λ_L and λ_B when the structure is subjected to strain. The result shows different linear responses

of (λ_B) and (λ_L) with slope sensitivities of -1.78 pm/με and -1.49 pm/με, respectively. The photo-elastic effect is dominant then a negative response was observed.

Fig. 4 shows the temperature response of the structure and a linear behavior was also obtained. The sensitivities are 38.4pm/ºC and 6.6pm/ºC for (λ_B) and (λ_L) respectively. A positive response is observed due to high dependence of the thermal expansion coefficient (pure silica).

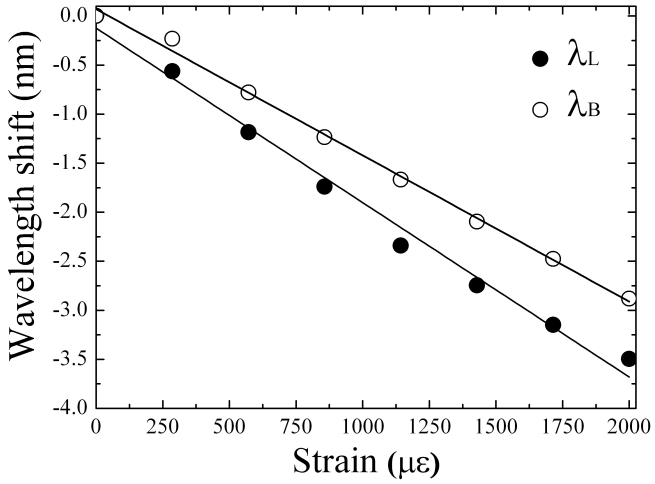

Fig. 3. Wavelength shift as a function of strain change for the wavelengths $\lambda_L$and λ_B.

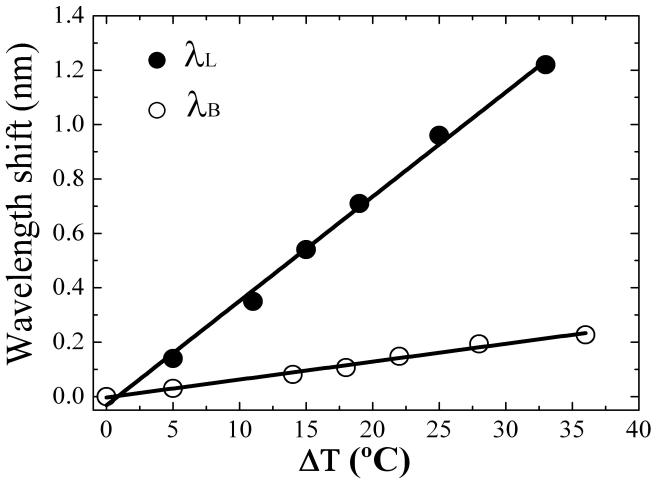

Fig. 4. Wavelength shift as a function of temperature change for the wavelengths λ_L and λ_B.

In order to sense the strain change $\Delta\varepsilon$ and temperature change ΔT, independent and simultaneously, the wavelength shift was recorded as $\Delta\lambda_B$ and $\Delta\lambda_L$, respectively, by an optical spectrum analyzer (OSA). These quantities can be expressed in terms of the strain change $\Delta\varepsilon$ and temperature change ΔT as follows:

$$\Delta\lambda_B(\varepsilon,T) = K_\varepsilon \Delta\varepsilon + K_T \Delta T \tag{1}$$

One can observe that K_T and K_ε are distinct when monitoring λ_B or λ_L, enabling the simultaneous measurement methodology which yields two linear equations whose matrix form is:

$$\begin{bmatrix} \Delta\lambda_B \\ \Delta\lambda_L \end{bmatrix} = \begin{bmatrix} K_{\varepsilon B} & K_{TB} \\ K_{\varepsilon L} & K_{TL} \end{bmatrix} \cdot \begin{bmatrix} \Delta\varepsilon \\ \Delta T \end{bmatrix} \tag{2}$$

where, $K_{\varepsilon B}$ and $K_{\varepsilon L}$ are the strain sensitivities, while K_{TB} and K_{TL} are the temperature sensitivities of λ_B and λ_L, respectively. In order to efficiently discriminate the temperature and the strain contributions, the matrix of coefficients K must be well conditioned. The relative values $\Delta\varepsilon$ and ΔT are obtained by the following equation:

$$\begin{bmatrix} \Delta\varepsilon \\ \Delta\mathrm{T} \end{bmatrix} = \frac{1}{45.468} \begin{bmatrix} 6.6 & -38.4 \\ 1.49 & -1.78 \end{bmatrix} \begin{bmatrix} \Delta\lambda_B \\ \Delta\lambda_L \end{bmatrix} \tag{3}$$

where the wavelength shifts $\Delta\lambda_L$ and $\Delta\lambda_B$ are expressed in picometers (*pm*), the strain variation ($\Delta\varepsilon$) is microstrain ($\mu\varepsilon$) and the temperature variation (ΔT) is in Celsius degrees (ºC). The root-mean-square (*rms*) deviations relative to the applied values are ±2 ºC and ±11 με for temperature and strain, respectively, which can be considered the resolutions obtained with this structure when implementing measurement of these two parameters simultaneously.

3. CONCLUSIONS

In conclusion, an all-fiber loop mirror using a clover microstructured fiber for simultaneous measurement of temperature and strain has been reported. The clover fiber has a rectangular core with an air-hole defect and this structure in the ring layout originates interference features that show different sensitivities to strain and temperature. Applying the matrix method it was possible to discriminate both parameters. Resolutions of ±2 ºC and ±11 με for temperature and strain, respectively, could be attained.

ACKNOWLEDGMENTS

This work was supported in part by the European COST action TD1001 and the Spanish Government project TEC2010-20224-C02-01.

REFERENCES

[1] Mortimore, D. B., "Fiber Loop Reflectors", Journal of Lightwave Technology 6(7), 1217–1224 (1988).
[2] Wang, Y., Zhao, C.-L., Dong, X., Kang, J., and Jin, S., "A fiber loop mirror temperature sensor demodulation technique using a long-period grating in a photonic crystal fiber and a band-pass filter," Review Of Scientific Instruments 82(7), art. no. 073101 (2011).
[3] Liu, Y., Liu, B., Feng, X., Zhang, W., Zhou, G., Yuan, S., Kai, G., and Dong, X., "High-birefringence fiber loop mirrors and their applications as sensors," Applied Optics 44(12), 2382-2390 (2005).
[4] Zhao, C-L., Yang, X., Lu, C., Jin, W., and Demokan, M.S., "Temperature-Insensitive Interferometer Using a Highly Birefringent Photonic Crystal Fiber Loop Mirror," IEEE Photonics Technology Letters 16(11), 2535-2537 (2004).
[5] Campbell, M., Zheng, G., Holmes-Smith, A.S., and Wallace, P.A., "A frequency-modulated continuous wave birefringent fiber-optic strain sensor based on a Sagnac ring configuration," Measurement Science and Technology 10(3), 218–224 (1999).
[6] Hatta, A.M., Semenova, Y., Wu, Q., and Farrell, G., "Strain sensor based on a pair of single-mode–multimode–single-mode fiber structures in a ratiometric power measurement scheme," Applied Optics 49(3), 536-541 (2010).
[7] Dong, B., Zhao, Q., Lvjun, F., Guo, T., Xue, L., Li, S., and Gu, H., "Liquid-level sensor with a high-birefringence-fiber loop mirror," Applied Optics 45(30), 7767–7771 (2006).
[8] Kim, K.-J., Yeom, S.-H., Kang, B.-H., Kim, D.-E., and Kang, S.-W., "Micro-optic Mach-Zehnder interferometric sensor for UV detection using photochromic dye," Sensor Letters 9(1), 195-198 (2011).
[9] Silva, S., Frazão, O., Viegas, J., Ferreira, L.A., Araújo, F.M., Malcata, F.X., and Santos, J.L., "Temperature and strain-independent curvature sensor based on a singlemode/multimode fiber optic structure," Measurement Science and Technology 22(8), 085201 (6pp) (2011).
[10] André, R.M., Marques, M.B., Roy, P., and Frazão, O., "Fiber Loop Mirror Using a Small Core Microstructured Fiber for Strain and Temperature Discrimination," IEEE Photonics Technology Letters 22(15), 1120-1122 (2010).
[11] Zhou, D.-P., Wei, L., Liu, W.-K., Liu, Y., and Lit, J.W.Y., "Simultaneous measurement for strain and temperature using fiber Bragg gratings and multimode fibers," Applied Optics 47(10), 1668-1672 (2008).